Jianlan Lu[1*]

Gas Emission Characterization and Monitoring Algorithm in the Process of Agricultural Waste Resource Treatment

Journal of Electrical Systems

Abstract: - To ensure that there is enough food produced for a growing population, trends in population growth and food consumption must be monitored. Therefore, farmers adopt various strategies without taking into account their detrimental effects on the surroundings to fulfil the necessary requirements. These kinds of actions frequently result in higher emissions of greenhouse gases . The use of fertilizer, soil, animals, and other factors all contribute to GHGs in the agriculture sector. In this Manuscript, Gas emission characterization and monitoring algorithm in the process of agricultural waste resource treatment (GECMA-AWRT-RDCNN)is proposed. Initially, the data is collected from Agri-food CO2 emission dataset. Then, the collected data is fed into pre-processing utilizing Implicit Bulk‐Surface Filtering (IBSF). The IBSF is used for data cleaning. Then the preprocessed data undergoes feature selection process. Here, it selects 14 features by utilizing High Level Target Navigation Pigeon Inspired Optimization (HLTNPIO). Then the selected features are given to Robust Deformed Convolutional Neural Network (RDCNN) for predicting Gas Yield (GY) generated by energy recovery from agricultural waste. RDCNN often does not explain techniques for optimising parameters through adaptation. Hence, the Fractional Order Water Flow Optimizer(FOWFO)to optimize Robust Deformed Convolutional Neural Network which accurately predict the Gas Yield. The proposed GECMA-AWRT-RDCNN approach is implemented in Python. The proposed method's performance examined utilizing performance metrics likes Accuracy, Mean-squared error (MSE), Root mean squared error (RMSE), Mean bias error (MBE), Determination coefficient , Relative root mean squared error (rRMSE), ,Mean absolute percentage error (MAPE) and Loss. The proposed GECMA-AWRT-RDCNN approach contains 28.0%, 27.5%, and 26.5% higher accuracy, 26.0%, 23.5%, and 28.5% higher Determination Coefficient and 12.0%, 17.5%, and 16.5% lower Mean Squared Error compared with existing methods, such as Electricity production based forecasting of greenhouse gas emissions in Turkey with deep learning, support vector machine and artificial neural network algorithms (EP-GHGE-SVM) Prediction of Agricultural Emissions in Malaysia Using Machine Learning Algorithms (PAEM-ARIMA) and Role of deep learning for prediction of greenhouse gas emission from agriculture: enabling technology (PGHGA-LSTM), respectively.

Keywords: Agricultural Waste, Fractional Order Water Flow Optimizer, Gas Emissions, High Level Target Navigation Pigeon Inspired Optimization, Implicit Bulk‐Surface Filtering and Robust Deformed Convolutional Neural Network.

I. INTRODUCTION

The agriculture sector contributes to climate change through anthropogenic greenhouse gas emissions [1]. The earth's surface emits heat energy, which greenhouse gases absorb and reradiate back, creating the greenhouse effect that leads to global warming. Numerous factors, such as altered average temperatures, altered rainfall patterns, an increase in floods and droughts, rainstorms, and fluctuations in sea level rise, are all impacted by climate change and have an impact on agriculture [2-4]. Ground level ozone concentrations and atmospheric carbon dioxide are both impacted by climate change. As the average temperature rises, crop productivity in quantity and quality suffers, as do growth rates. Greenhouse Gas (GHG) emissions are on a historic climb. GHG emissions are creating climate change, leading to rising surface temperatures [5-7]. The IPCC estimates that between 1880 and 2012, land-ocean temperatures rose globally by 0.85 °C. The IPCC claims that the temperatures between 1983 and 2012 were the highest in 800 years. Nitrous oxide (3-7%), carbon methane (4-9%), Water vapour (36-70%), dioxide (9-26%), HFC, and SF6 are the six gases that are classified as greenhouse gases. The IPCC ranks methane as the second most significant contributor to global warming, accounting for 21-25%.The agricultural sector accounts for around 25% of global GHG emissions. With a rapidly expanding global population, there is a pressing need for increased food production [8-11]. Livestock emit methane as part of their digestion process. It is generated by the rumen of animals [12-14]. It promotes microbial activity and produces incombustible gasses. Ruminants' enteric fermentation contributes to 15-18% of methane emissions [15, 16]. Studies indicate that 19.9 GtCO2 is the approximate amount of emissions resulting from land utilisation, forestry, and agriculture. Fertiliser with nitrogen produces an additional 0.4 GtCO2 emissions. The primary sources of agricultural emissions are fertiliser (0.6 GtCO2), manure (1.8 GtCO2), on-farm energy (1.0

[1] [1*]Lecturer, Jiangsu Vocational College of Agriculture and Forestry, Jurong, Jiangsu, China, 212400

[1*]Email: jianlanluphd@gmail.com

GtCO2), rice cultivation (2.1 GtCO2), and enteric fermentation (8.3 GtCO2) [17, 18]. The need for additional food, especially protein, is rising as the world's population gets closer to 10 billion [19]. Given the current rate of deforestation, emissions are expected to grow by approximately 23.4 GtCO2 by 2050. According to a 2018 IPCC study, significant change is needed to keep global warming to 1.5 degrees Celsius [20].

Limitation of the previous research is the narrow scope of input variables and waste treatment technology. The research only looked at input variables for estimating gas yield from agricultural waste, which may have overlooked other key aspects that could have an impact on prediction accuracy. The model's predictive powers may be limited by ignoring key variables that may have a substantial impact on gas yield, resulting in potential mistakes in gas production estimates. For gas yield prediction, without investigating its applicability in other waste treatment processes such as biological gasification. This narrow emphasis may limit the findings' application to a larger range of waste management settings.

To overcome the limits of the research, the input variables examined in the prediction model can be expanded to include a broader spectrum of factors influencing gas yield. The chief aim of the research is to create and suggest a model for gas yield prediction using the FOWFO algorithm and the RDCNN model. While the local minimum can increase an RDCNN model's performance by identifying a better way to train the network, choosing and calculating the ideal weights and biases remains difficult for RDCNN. On the other hand, for optimization issues, the FOWFO algorithm can carry out a global optimization. Therefore, the GECMA-AWRT-RDCNN model, which is an RDCNN model, has its weights optimized using the FOWFO algorithm. The sections that follow provide a description of the GECMA-AWRT-RDCNN model's framework for forecasting gas yield.

Below is a summary of this research work's principal contributions.

- In this research, Gas emission characterization and monitoring algorithm in the process of agricultural waste resource treatment (GECMA-AWRT-RDCNN)is proposed.
- Initially the input image is collected from the Agri-food CO2 emission dataset.
- The proposed GECMA-AWRT-RDCNN method integrates multiple advanced techniques, including Implicit Bulk‑Surface Filtering (IBSF) for preprocessing. The preprocessed image undergoes feature selection using HLTNPIO.
- Then the selected 14 features are given to Robust Deformed Convolutional Neural Network (RDCNN) for predicting Gas Yield.
- Unlike traditional RDCNN approaches, which lack optimization methods for computing optimal parameters, the proposed method incorporates Fractional Order Water Flow Optimizer (FOWFO).FOWFO optimizes the weight parameters of RDCNN.
- The effectiveness of the proposed approach is examined using current techniques, like CM-PGHGA-LSTM, PAEM-ARIMA and EP-GHGE-SVM models respectively.

The remaining manuscripts are arranged as follows: The literature review is reviewed in Part 2, the technique is explained in Part 3, the results are verified in Part 4, and the article is concluded in Part 5.

II. LITERATURE SURVEY

Several works have presented previously in literatures were depending on the prediction ofgas yieldusing deep learning. Few of them were mentioned here,

Kosamkar and Kulkarni [21] have presented a PGHGA-LSTM .The agriculture sector adds to GHS emissions through cattle, soil, and fertilizer use. An extensive examination of greenhouse gas emissions from the agriculture sector is provided in this research. The research found a link between agricultural activities such as land utilization, nitrogen fertiliser application, and GHG emissions from agriculture. Suggested architecture uses an LSTM deep learning model to analyze and predict greenhouse gas emissions from agriculture. The disadvantage of this method was that it may oversimplify complex agricultural systems and rely too heavily on technology while failing to address broader socioeconomic and policy aspects influencing emissions. This method attains high loss and low accuracy.

Homaira and Hassan[22] have presented a PAEM-ARIMA. Developing a model that predicts agricultural emissions using the 3 most dependable forecasting techniques was the aim of this study. Two models are used in the time series analysis: a simple linear regression model and the ARIMA and LSTM. Malaysia's predicted growing trend values are displayed in these models until 2040. While the LSTM model produced a diminishing

curve for each value loss epoch, suggesting that it was a poor forecasting model, the ARIMA model produced strong prediction curves that were close to the real values recorded since 1960. The disadvantage of this strategy was that it may focus too heavily on technical solutions without adequately addressing broader socioeconomic or policy factors driving agricultural emissions. This method attains high Mean-squared error and low Determination Coefficient.

Bakay and Ağbulut [23] have presented an EP-GHGE-SVM alogrithm. Fossil fuels currently provide for 85% of the world's primary energy needs. The widespread usage of fossil-based fuels has resulted in an increasing release of GHG over the world. The power and heat generating industry accounts for the majority of overall GHG emissions (25%). This research aims to anticipate GHG emissions (N2O, CH4 F-gases, total GHGand CO2) from Turkey's electricity generating sector using ANN, DL, and SVM. The Turkish Statistical Institute contributed the dataset, which spans the years 1990–2018.The method may overlook broader contextual elements influencing emissions and energy production. This method attains high Loss and low Determination Coefficient.

Nielsen et al. [24] have presented how geochemistry is related to soil GHG emissions from agricultural bare peat mesocosms that have been drained and rewetted.. Rh emissions in five Danish fens and bogs are shown to be driven by soil and site-specific geochemical components. Additionally, it looks at emission magnitudes in both drained and rewetted scenarios. A mesocosm experiment was carried out with water table depths adjusted to -40 cm or -5 cm, and equivalent exposure to climatic conditions. Overall, evaluations employing generalized additive models (GAM) revealed that geochemical variables adequately described emission magnitudes. Soil pH and phosphate (P) were significant predictors of CO2 flux magnitudes under drained circumstances. This research may limit its applicability to real-world situations, perhaps disregarding larger biological and climatic aspects impacting peat land GHG emissions. This method attains high Relative root mean squared error and low accuracy.

Raihan et al. [25] have presented an econometric study of Bangladesh's greenhouse gas emissions resulting from several agricultural variables. Due to its impact on greenhouse gas emissions, agriculture contributes significantly to environmental degradation and was particularly vulnerable to Climate Variability. Thus, the current study experimentally investigates the dynamic relationships between GHG emissions in Bangladesh and agricultural value added, agricultural land expansion, crop output, animal and fisheries production, agricultural energy usage, fertiliser use, and forest area. Time series data covering the years 1990 to 2018 were analyse This approach may overlook deeper systemic difficulties and relies primarily on statistical correlations, thus leaving out socioeconomic and policy factors critical for effective emission reduction initiatives.This method attains high Root mean squared error and low accuracy.

Gołasa et al.[26] have presented a Agriculture's Sources of Greenhouse Gas Emissions, with a Focus on Emissions from Energy Used. The economic sector most impacted by the recent changes was agriculture. Being a significant source of GHG emissions, the necessity to reduce these emissions was becoming more and more apparent. The purpose of the research was to assess the structure of GHG emissions on farms and to pinpoint the kinds of farms where GHG emissions may be decreased by improved energy management, using data from the FADN. The IPCC methodology was modified for use with FADN data in order to compute the emission volume. When compared to other emission sources, energy production was determined to have very low emissions. The methods may oversimplify emission reduction efforts by focusing primarily on farm types, potentially ignoring broader systemic variables and taxation's socioeconomic implications. This method attains high MBE and low MAPE .

Sharafi et al. [27] have presented an estimate of the amount of energy used and GHG emissions in crop production. A ML approach. In order to evaluate the long-term energy efficiency of essential crops, the research gathers and analyses energy inputs and GHG emissions from 17 Iranian crops in 5 main categories (tubers, pulse fibre, cereal and oilseed) from 1970 to 2019. To quantify the link between GHG emission models and the resources utilised per unit of energy output, three machine learning (ML) techniques were developed. Three numerical statistics were used to assess the models. Every physical and chemical input required to produce the principal crops is considered in the study. These energy-related factors include manpower, irrigation water ,equipment, electricity, fossil fuels, pesticides, fertilisers (nitrogen, phosphate and potassium), and seed rate .The method may overlook important socioeconomic and environmental elements that influence energy

efficiency and emissions, thus leading to oversimplified models and solutions. This method attains high mean bias error and low Determination coefficient.

III. PROPOSED METHODOLOGY

In this segment, Gas emission characterization and monitoring algorithm in the process of agricultural waste resource treatment (GECMA-AWRT-RDCNN) is proposed. The approach involves five steps: Data Acquisition, Pre-processing, feature selection, prediction and optimization. The process begins with the acquisition of Agri-food CO2 emission dataset, a crucial step in ensuring the availability of reliable and relevant data for analyses. Following Data acquisition, the data's undergo pre-processing using an Implicit Bulk‑Surface Filtering (IBSF)for data cleaning. In the Feature selection stage, the HLTNPIO is used to choose features from the pre-processed data. The selected 14 features are then input into a Robust Deformed Convolutional Neural Network (RDCNN)for the purpose of prediction. The RDCNN, known for its robustness and ability to handle complex data, is tasked with the critical role of prediction. By leveraging its deep learning capabilities, the RDCNN predict the gas yield (GY) generated by energy recovery from agricultural waste. To further enhance the performance of the RDCNN and optimize its parameters for improved accuracy and efficiency, the FOWFO technique is employed. Proposed GECMA-AWRT-RDCNN block diagram is illustrated in figure 1.

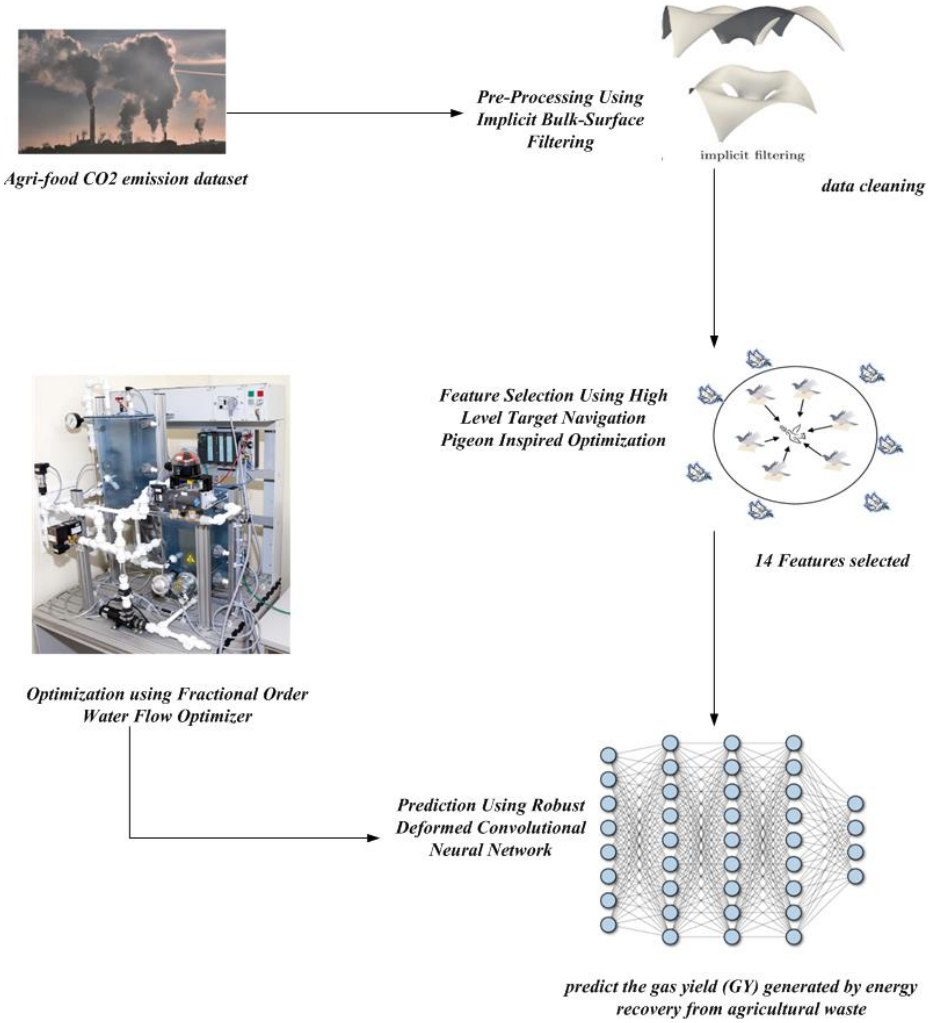

Figure 1: Proposed GECMA-AWRT-RDCNN block diagram

A. Data Acquisition

Firstly, the input data's are collected from Agri-food CO2 emission dataset [28].The FAO and the IPCC provided data, and these sources were combined and reprocessed to create the agricultural CO2 emission dataset. To produce a thorough and coherent dataset for analysis and forecasting, these datasets were cleaned, preprocessed, and combined. The dataset, as shown in the notebook, details the CO2 emissions associated with

agri-food, which make up about 62% of all annual emissions worldwide. In fact, when researching climate change, the emissions from the agri-food industry are important. These emissions add significantly to the annual emissions worldwide, as the dataset demonstrates. In order to mitigate climate change and establish sustainable practices within the agri-food industry, it is imperative to comprehend and address the environmental impact of this sector. Table 1 shows the features of Agri-food CO2 emission dataset.

Table 1: List of features Agri-food CO2 emission dataset

Sl.No	Features	Sl.No	Features
1	Savanna fires	13	Forest fires
2	Crop Residues	14	Rice Cultivation
3	Drained organic soils (CO2)	15	Pesticides Manufacturing
4	Food Transport	16	Forestland
5	Net Forest conversion	17	Food Household Consumption
6	Food Packaging	18	Agrifood Systems Waste Disposal
7	Food Processing	19	Fertilizers Manufacturing
8	IPPU	20	Manure applied to Soils
9	Manure left on Pasture	21	Manure Management
10	Fires in organic soils	22	Fires in humid tropical forests
11	Food Retail	23	On-farm Electricity Use
12	On-farm energy use	24	total_emission

B. Pre-Processing Using Implicit Bulk-Surface Filtering(IBSF)

In this section, pre-processing using Implicit Bulk-Surface Filtering (IBSF) [29] is discussed. In the preprocessing, IBSF is used for data cleaning. By integrating bulk and surface measurements, Implicit Bulk-Surface Filtering (IBSF) improves gas emission monitoring in the treatment of agricultural waste. Its capacity to preserve volume mesh quality and guarantee surface smoothness at the same time is important when discussing gas emission in the treatment of agricultural waste. By taking a comprehensive approach, gas emission dynamics modeling becomes more accurate and computationally efficient. This leads to more accurate assessments of emission patterns and more efficient waste treatment process development. In agricultural waste treatment plants, it supports efficient decision-making for environmental management and regulatory compliance by ensuring strong and trustworthy numerical computations.

$$-(r_{\Omega}^{H})^{2}\nabla.\sigma + x = s, \qquad in\ \Omega \tag{1}$$

Here ∇ represent the conventional spatial gradient operator, x represent the generalized Robin boundary condition , r_{Ω}^{H} represent the Helmholtz bulk filter radius,, σ represent an equivalent 2nd order tensor to continuum mechanics' Cauchy stress tensor, and s represent the partial differential equation.

$$\sigma = \lambda\, tr(\varepsilon(x))I + 2\mu\,\varepsilon(x) \tag{2}$$

Here ε indicates the tensor of strain operating on geometry, λ and μ are the Lame constants, tr represent the trace operator, , I represent the identity tensor.

$$\Pi(x) = \frac{1}{2}(r_{\Omega}^{H})^{2}\int_{\Omega}\sigma:\varepsilon\, d\Omega + \frac{1}{2}(r_{\Gamma}^{H})^{2}\int_{\Gamma}\nabla_{\Gamma}x^{T}.\nabla_{\Gamma}yxd\Gamma \tag{3}$$

Where $(r_{\Omega}^{H})^{2}$ and $(r_{\Gamma}^{H})^{2}$ represent the corresponding weights, Ω represent the geometry's overall strain energy, A uniform distribution throughout the integration domains is assumed by $d\Gamma$ and $\nabla_{\Gamma}x^{T}$ represent the smoothness of the design boundary.

$$(r_{\Omega}^{H})^{2} = \beta\frac{(r_{\Gamma}^{H})^{2}\int_{\Gamma}\nabla_{\Gamma}x^{T}.\nabla_{\Gamma}xd\Gamma}{\int_{\Omega}\sigma:\varepsilon\, d\Omega},\ 0<\beta\le 1 \tag{4}$$

Where β represent the weighting factor. $d\Omega$ indicates the geometry's overall strain energy. r_{Ω}^{H} represent the Helmholtz bulk filter radius, $\nabla_{\Gamma} x^{T}$ represent the smoothness of the design boundary. σ represent an equivalent 2nd order tensor to continuum mechanics' Cauchy stress tensor. Data is cleaned in equation (5)

$$K_{\Omega} = \sum \int_{\Omega^e} \left(r_{\Omega^e}^{H}\right)^2 B^T C B \, d\Omega \tag{5}$$

Where C represent the isotropic constitutive matrix that is linear-elastic. The bulk shape functions N spatial gradients are contained in B. $r_{\Omega^e}^{H}$ represent the elemental Helmholtz bulk filter radius. Finally, the IBSF cleaned the data. Then, the pre-processed output is fed to HLTNPIO for Selecting Features.

C. Feature Selection UsingHigh Level Target Navigation Pigeon Inspired Optimization (HLTNPIO)

In this section, the feature selection using HLTNPIO [30] is discussed. An effective strategy for improving gas emission management in the treatment of agricultural waste is provided by the cutting-edge ideas incorporated into HLTNPIO. By improving worldwide search capabilities, striking a balance between exploitation and exploration, and promoting the synergistic evolution of solutions, HLTNPIO makes it possible to manage gas emissions more effectively and adaptively, which eventually helps agricultural waste treatment processes comply with regulations and the environment.

Step 1: Initialization

The starting population of HLTNPIO is generated randomly. Then the initialization is derived in equation (6).

$$T_{i,d}^{ini} = B_{\min} + rand \cdot \left(B_{\max} - B_{\min}\right) \tag{6}$$

Where $B_{\max}$ and $B_{\min}$ denotes the bound's maximum value and minimum value, respectively.

Step2: Random Generation

Following startup, HLTNPIO caused the input fitness function to become random.

Step 3: Fitness Function

Based on the present best position , the initialised parameters are determined. Determine the fitness level of every person.

$$Fitness\ function = [\ Selecting\ \ Optimal\ \ Features\ ] \tag{7}$$

Step 4:Selection

The first strategy's final phase, selection, attempts to separate high-level targets from intermediate targets. Since the target group is a changing population, it is necessary to replace outdate targets with more suitable ones. The following operations are carried out by the selection component to weed out the ultimate targets.

$$T_i^{t+1} = \begin{cases} T_i^t, & f\left(T_i^t\right) < f\left(MT_i^t\right) \\ MT_i^t, & f\left(T_i^t\right) \geq f\left(MT_i^t\right) \end{cases} \tag{8}$$

Where $f\left(T_i^t\right)$denotes the i^{th} target's fitness value in the t^{th} generation . $f\left(MT_i^t\right)$denotes the i^{th} intermediate target's fitness value in the t^{th} generation . T_i^t denotes the $(t+1)-th$generation's i^{th} objective.

Step 5: Levy Based Map Compass Strategy

Pigeons fly toward objectives in the LMS and investigate possible locations nearby. Based on PIO's original map compass strategy, LMS has been modified. Second, the LMS's random search functionality is improved by introducing the Levy flight model.

$$V_{i,d}^{t+1} = V_{i,d}^{t} + rand \cdot \left(T_{i,d}^{t} - X_{i,d}^{t}\right) \tag{9}$$

Where T_i represents the ith high level target, V_i denotes the ith pigeon's velocity , $rand$ denotes the random number and X_i represents the ith pigeon's position with d dimension search space.

$$X_{i,d}^{t+1} = T_{i,d}^{t} \times \left(1 - e^{-R_{i,d\cdot t}^{t}}\right) + \chi \cdot V_{i,d}^{t+1} \tag{10}$$

Where $R_{i,d}^{t}$ represents the map-compass factor of the i^{th} pigeon in the t^{th} generation's dth pigeon variable, V_i denotes the the ith pigeon's velocity , $T_{i,d}$ represents the ith high level target with d dimension search space, χ denotes the levy flight step length and $X_{i,d}$ represents the ith pigeon's position with d dimension search space,

Step 6: Enhanced Landmark Strategy

PIO accelerated convergence in the latter search stage and improved local exploitation capabilities by utilising the map-compass technique. The centre of the existing population is designated as the landmark in the first map-compass method of PIO, all pigeons fly towards it, and the population is gradually reduced. Although this approach is effective in utilizing precise solutions, it lessens population variety. In order to solve the issue, ELS chooses a subset of the targets' elites and uses their canters as landmarks to guide the pigeons' movements rather than using the population's center as a reference point.

$$V_{i,d}^{t} = V_{i,d}^{t-1} + rand \cdot \left(T_{i,d}^{t} - X_{i,d}^{t-1}\right) + rand \cdot \left(C_{e}^{t} - X_{i,d}^{t-1}\right) \quad (11)$$

Where $V_{i,d}$ denotes the velocity of the ith pigeon with d dimension search space, $rand$ denotes the random number, $T_{i,d}$ represents the ith high level target with d dimension search space, $X_{i,d}$ represents the ith pigeon's position with d dimension search space, d represents the current dimension , i denotes the current pigeon number, and C_e^t represents the center position of the elites.

Step 7: Termination

In this step, HLTNPIO completes, best solution obtained through each process iterations returned as output. HLTNPIO selected 14 features from Agri-food CO2 emission dataset. Then the selected features are given to RDCNN. Selected features from Agri-food CO2 emission dataset shown in table 2.

Table 2: Selected Features

Sl.No	Features	Sl.No	Features
1	Drained organic soils	8	Pesticides Manufacturing
2	Food Transport	9	Forestland
3	Net Forest conversion	10	Food Household Consumption
4	Food Packaging	11	Agrifood Systems Waste Disposal
5	Fires in organic soils	12	Fires in humid tropical forests
6	IPPU	13	On-farm Electricity Use
7	On-farm energy use	14	total_emission

D. Prediction UsingRobust Deformed Convolutional Neural Network (RDCNN)

In this section Robust Deformed Convolutional Neural Network (RDCNN) [31] is utilized. RDCNN is used to predict Gas Yield (GY) generated by energy recovery from agricultural waste. A powerful tool for improving gas emission characterization and monitoring in agricultural waste treatment, the Robust Deformed Convolutional Neural Network (RDCNN) offers significant advantages in gas emission characterization and monitoring for agricultural waste treatment. Its deformed convolutional layers allow for the capture of intricate patterns in emission data, enhancing accuracy. Additionally, RDCNN's robustness to variability ensures consistent performance across diverse conditions, which is crucial given the often-variable nature of agricultural waste treatment processes.

$$Q(\theta) = \frac{1}{2m}\sum_{j=1}^{m}\left\| RDCNN\left(Q_m^j\right)\right\| \quad (12)$$

Where $Q(\theta)$ represents the loss function, m represents the geometric reshaping capability, $RDCNN$ represents the robust deformed convolutional neural network, Q_m^j adjust position of the sampling point.

$$Q_{DB} = DB(Q_m) = 11BCR(Q(DC(Q_m))) \quad (13)$$

Where Q_{DB} represents the output of DB, DB represents the deformable block, Q_m represents the low computation time in contextual information, $11BCR$ represents the eleven stacked deformable block, Q represents the input adjust position, C represents the reshaping capability, D represents the improved clarities.

$$X\left(j_{x,}j_{y}\right)=\sum_{a=1}^{m}Y\left(j_{x,}j_{y},a\right)G\left(j_{y}+\Delta y_{a}+\Delta y\right) \tag{14}$$

Where X represents the obtained features, $j_{x,}j_{y}$ represents the location of the centre point, Y represents the obtained feature map, a represents the convolutional operation, G represents the total number of pixels obtained from features, Δy_a denotes the offset, Δy represents the horizontal offset.

$$Q_{BD}=\alpha\ EB\left(Q_{BD}\right) \tag{15}$$

Where Q_{BD} denotes the original images, α represents the high accuracy adjust position of the images, EB represents the elastic block, $BE\left(Q_{BD}\right)$ represents the output of the original images. Gas Yield is predicted in equation (16)

$$R_{d}=QN\left(O_{EB}\right) \tag{16}$$

Where R_d represents the forged images, Q represents the residual block, N represents the residual operation, O_{EB} represents the latent clean image. Finally, Gas Yield (GY) generated by energy recovery from agricultural waste is predicted using RDCNN. In this work, FOWFO is assigned to enhance RDCNN. Here, FOWFO is assigned for turning weight parameter of RDCNN.

E. Optimization using Fractional Order Water Flow Optimizer(FOWFO)

In this segment, FOWFO [32] is discussed. It determines the parameters such as $Q_{BD}\ and\ R_d$ .The FOWFO-based technology assists in reducing environmental concerns related to the treatment of agricultural waste by precisely defining and tracking gas emissions. It makes sure that harmful emissions are kept to a minimum, which promotes sustainability and environmental preservation. When compared to conventional control techniques, the fractional order control mechanisms used by FOWFO offer more resilience and flexibility.

Step 1: Initialization

The starting population of FOWFO is generated randomly. Then the initialization is derived in equation (17).

$$H=\begin{bmatrix} H_{\min} & H_{\max}^{1} & \ldots.. & H_{i}^{1} \\ H_{\min}^{2} & H_{\max}^{2} & \ldots.. & H_{i}^{2} \\ . & . & . & . \\ H_{\min}^{n} & H_{\max}^{n} & \ldots.. & H_{i}^{n} \end{bmatrix} \tag{17}$$

Where, $(H_{\min})$ is the minimum value that the initialize current solution of (H) at iteration (t) can achieve while $(H_{\max})$ is the maximum possible attainable value that can be achieved.

Step 2: Random Generation

Through FOWFO, the input fitness function acquired randomization upon initialization.

Step 3: Fitness Function

Based on the current best position , the initialised parameters are resolved. Determine each person's fitness value.

$$Fitness\,Function=optimize(Q_{BD}\ and\ R_{d}) \tag{18}$$

Where R_d is used to reduce the MSR and Q_{BD} is used to increase the accuracy.

Step 4: Enhancement the Laminar Operator of Water Flow Optimizer Q_{BD}

FO is added to the laminar operator during the exploitation stage by exchanging information across solutions, making use of its memory characteristic for previous events to improve the accuracy and convergence speed of the solution.

$$C'[Y_{i}(l+1)]=Y_{j}(l+1)-Y_{j}(l)=v*\vec{c} \tag{19}$$

Where C' represent the position of the particle, Y_i represents the shifting coefficient, Y_j represents the random number, l represents the position of the particle chosen at random, v represents the direction of the moving particle, $*$ represents the laminar operator, $\vec{c}$ represents the constant.

$$C^{\in}[Y_j(l+1)] = v * \vec{c} \quad (20)$$

Where $C^{\in}$ represents the arbitrary phase. $*$ represents the laminar operator, $\vec{c}$ represents the constant.

Step 5: Linear Increase of Laminar Probability R_d

When Coef is low in the early stages of iteration, the algorithm is more likely to focus on global exploration. The algorithm is more prone to local exploitation at this later iteration since Coef has a large value. The entire procedure helps to maintain a balance between exploitation and exploitation.

$$Y_j^{l+1} = \frac{1}{1!} \in Y_j^l + \frac{1}{2!} \in (1- \in) Y_j^{l-1} + v * \vec{c} \quad (21)$$

Where Y_j^{l+1} represents the space among water surface, $\in$ represents the coefficient vector, Y_j^l represents the flowing water, $1- \in$ represents the sampling period, Y_j^{l-1} represents the number of terms from the previous events. Figure 2: shows Flowchart of FOWFO.

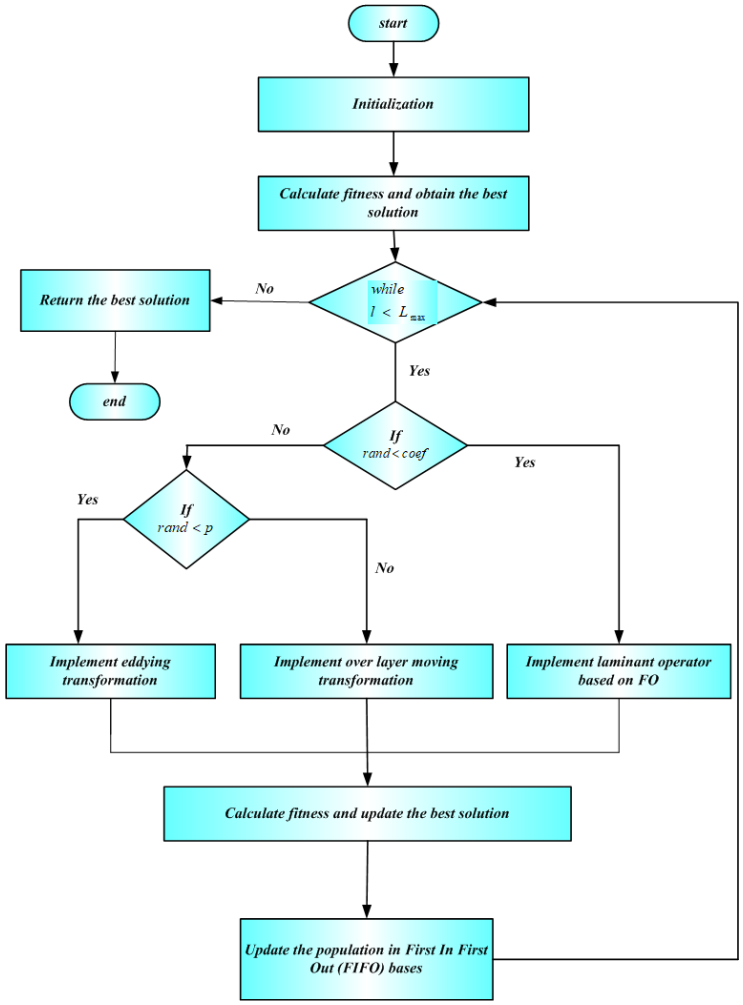

Figure 2: Flowchart of FOWFO

Step 6: Termination

In this stage, the weight parameter Q_{BD} *and* R_d of Robust Deformed Convolutional Neural Network are optimized with the help of FOWFO, iteratively repeat the step 3 until the halting is $H = H + 1$ met. Then finally proposed GECMA-AWRT-RDCNN predicted thegas yield with higher accuracy.

IV. RESULT WITH DISCUSSION

This part discusses the results of the proposed technique. The proposed GECMA-AWRT-RDCNN method is then simulated in Python and compiled utilizing Jupiter notebook and executed in Mac Book Pro along Intel core i7 processor of 2.7 GHz, 8GB of RAM speed. The obtained outcome of the proposed GECMA-AWRT-RDCNN approach is analysed with existing systems like PGHGA-LSTM, PAEM-ARIMA and EP-GHGE-SVM respectively.

A. Performance Measures

Selecting the best classifier requires taking this critical step. Performance is evaluated using a variety of performance metrics, such as accuracy, MAPE, determination coefficient, MSE, RMSE, MBE, and rRMSE . Performance measurements are scaled using the judged performance metric. It is necessary to have True Negative (TN), False Positive (FP), and False Negative (FN) samples in order to scale the performance indicator, True Positive (TP).

1) Accuracy

Equation (22) provides the accuracy, which quantifies the percentage of samples (both positive and negative) relative to the entire samples.

$$Accuracy = \frac{TP + TN}{TP + TN + FP + FN} \tag{22}$$

2) Mean Squared Error (MSE)

The term "mean square error" refers to “the average of the squares of the errors” or variances between the actual and anticipated values in a dataset. The formula to calculate MSE is as follows:

$$MSE = \left(\frac{1}{n}\right) * \sum \left(x_i - \hat{x}_i\right)^2 \tag{23}$$

3) Root Mean Square Error (RMSE)

The two main metrics used to assess the efficiency of a regression model are its accuracy and its RMSE, which computes the average difference between values predicted by the model and values that actually occur. The accuracy of the model's prediction of the target value is estimated by it.

$$RMSE = \sqrt{\frac{\left(Actual\ Value - \mathrm{Pr}edicted\ Value\right)^2}{Number of\ observation}} \tag{24}$$

4) Mean Bias Error (MBE)

A statistic called MBE calculates the average difference between a dataset's actual and predicted values. The formula to calculate MBE is as follows:

$$MBE = \left(\frac{1}{n}\right) * \sum \left(x_i - \hat{x}_i\right) \tag{25}$$

5) Relative Root Mean Squared Error (rRMSE)

rRMSE is derived by dividing the RMSE by the average of the real values. It provides a normalized measure of the RMSE while accounting for the data's scale.

$$rRMSE = \left(\frac{RMSE}{mean\left(actual values\right)}\right) * 100 \tag{26}$$

6) Determination Coefficient

The Determination Coefficient (R^2) in a regression model represents how well the independent variables are able to predict the variance of the dependent variable. To calculate the Determination Coefficient (R^2), use the formula below:

$$R^2 = 1 - \left(SSres \big/ SStot\right) \tag{27}$$

Where $SStot$ indicates the total sum of squares and $SSres$ represent the sum of squares of residuals .

7) Mean Absolute Percentage Error (MAPE)

The MAPE is a metric for determining the accuracy of a forecasting model by measuring the average percentage difference between anticipated and actual values. The formula for computing MAPE is given below:

$$MAPE = \left(\frac{1}{n}\right) * \sum\left(\left| \left(Actual - Forecasted\right) \middle/ Actual \right| \right) * 100 \quad (28)$$

Here n represent the count of observations. $Forecasted$ represent the forecasted value.

8) Loss

The loss curve indicates the values of the model's loss over time. The loss is initially substantial but steadily lowers, demonstrating that the model's performance is increasing.

$$Loss = \frac{\left(Actual\ Value - \Pr edicted\ Value\right)^2}{Number\ of\ observation} \quad (29)$$

B. Performance Analysis

Figure 3 to 10 illustrates the simulation outcome of proposed GECMA-AWRT-RDCNN technique . Then, the proposed GECMA-AWRT-RDCNN technique is likened with existingPGHGA-LSTM, PAEM-ARIMA and EP-GHGE-SVMmethods respectively.

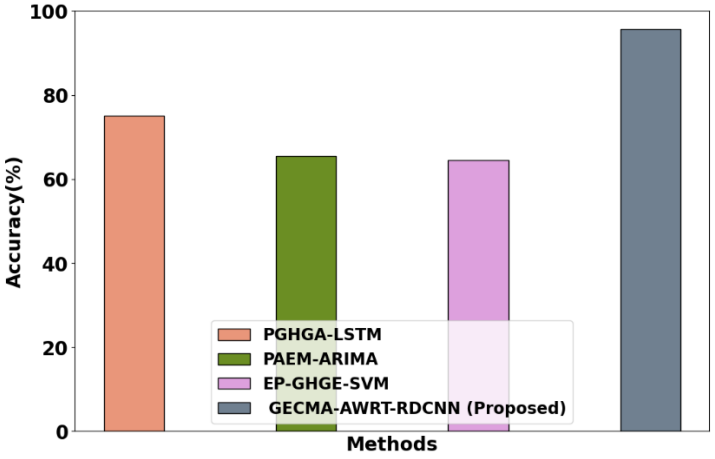

Figure 3: Performance Analyses of Accuracy

Figure 3 displays performance analyses of accuracy.The GECMA-AWRT-RDCNNmodel, optimized with the FOWFO method, demonstrated improved accuracy and predictive capacities in forecasting gas yield during the gasification of agricultural waste. The optimization procedure increased the RDCNNmodel's performance and contributed to more trustworthy GY predictions, emphasizing the importance of algorithmic optimization in boosting model accuracy. The proposed GECMA-AWRT-RDCNNmethod attains 28.0%, 27.5%, and 26.5%higheraccuracy estimated to the existing method such as PGHGA-LSTM, PAEM-ARIMA and EP-GHGE-SVM models respectively.

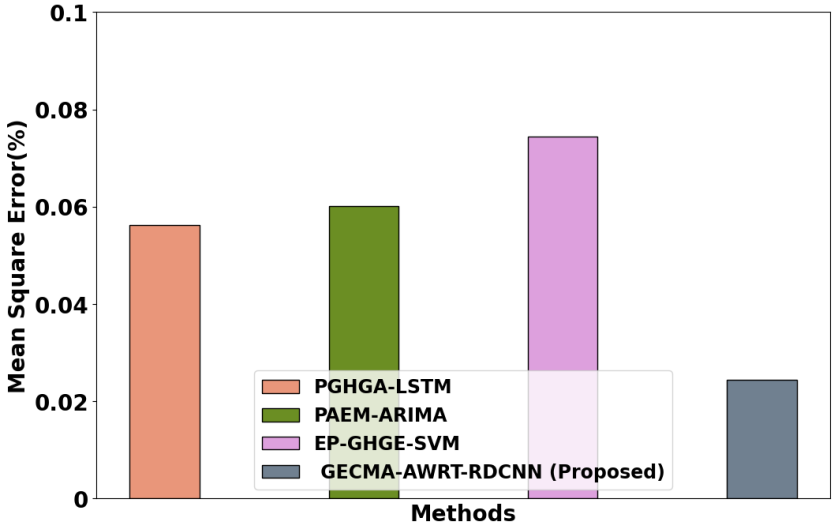

Figure 4: Performance Analysis of Mean Squared Error

Figure 4 displays performance analyses of Mean Squared Error. The MSE analysis demonstrated the effectiveness of the FOWFO algorithm in optimizing the RDCNNmodel for estimating gas output from municipal solid waste. The decrease in MSE values in the GECMA-AWRT-RDCNNmodel revealed the improved accuracy and predictive capacities acquired by algorithmic optimization, stressing the importance of MSE as a performance parameter in evaluating model accuracy and efficacy. The proposed GECMA-AWRT-RDCNNmethod attains 12.0%, 17.5%, and 16.5%lowerMean Squared Error estimated to the existing method such as PGHGA-LSTM, PAEM-ARIMA and EP-GHGE-SVM models respectively.

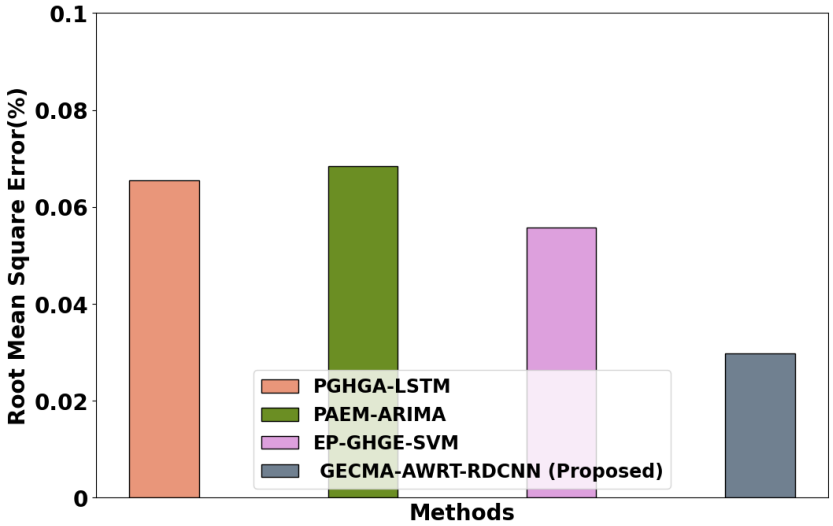

Figure 5: Performance Analyses of Root Mean Squared Error

Figure 5 illustrates performance analyses of Root Mean Squared Error.The RMSE performance graph for agricultural waste with percentages illustrates the forecasting model's accuracy in predicting agricultural waste quantities. It enables stakeholders to evaluate the model's performance, spot patterns in prediction mistakes, and make informed decisions based on RMSE values. Compare the RMSE percentages of various forecasting models or time periods to determine which one has the lowest RMSE percentage, suggesting the most accurate projections of agricultural waste levels. The proposed GECMA-AWRT-RDCNNmethod attains 17.0%, 14.5%, and 16.5%lower RootMean Squared Error estimated to the existing method such as PGHGA-LSTM, PAEM-ARIMA and EP-GHGE-SVM models correspondingly.

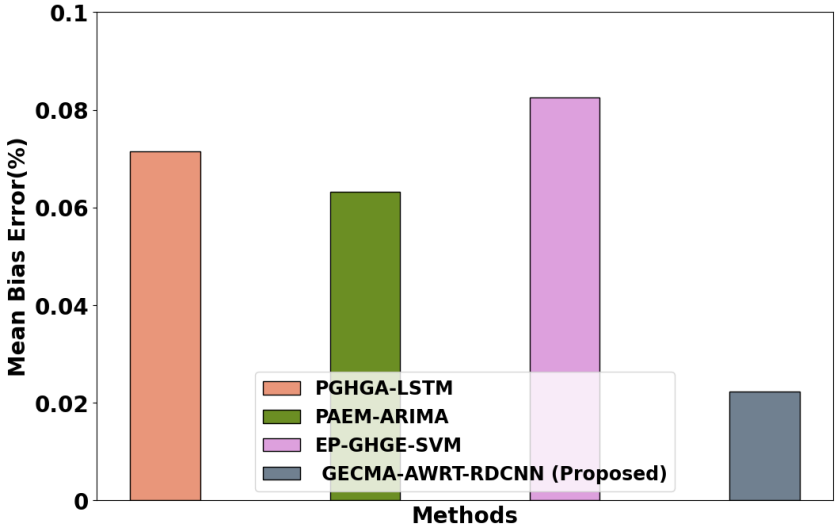

Figure 6: Performance Analyses of Mean Bias Error

Figure 6 illustrates performance analyses of Mean Bias Error.The MBE graph typically depicts MBE values over time or various data points pertaining to agricultural waste amounts. Each data point on the graph reflects the model's average bias or propensity as compared to the actual values for a given period or observation. Analyzing the MBE percentages in the graph provides insight into the direction and extent of bias in the model's estimates of agricultural waste quantities. Positive MBE percentages imply an overestimation bias, whilst

negative MBE numbers indicate an underestimate bias. The proposed GECMA-AWRT-RDCNNmethod attains 17.0%, 24.5%, and 11.5%lower Mean Bias Errorestimated to the existing method such as PGHGA-LSTM, PAEM-ARIMA and EP-GHGE-SVM models respectively.

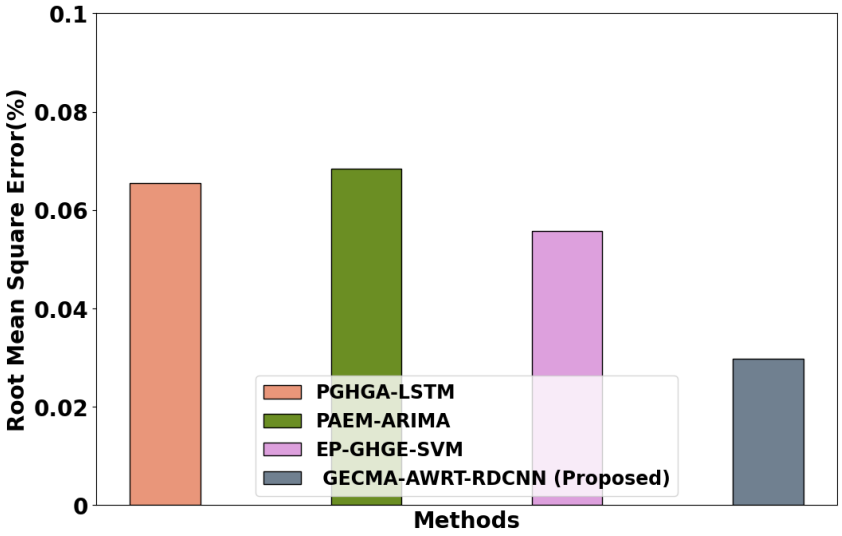

Figure 7: Performance Analyses of Relative Root Mean Squared Error

Figure 7 displays performance analyses of Relative Root Mean Squared Error.A lower rRMSE suggests greater performance since it indicates that the forecasting model has a less relative error than the mean actual values. Examining the trend of rRMSE percentages over time can reveal information about the consistency of relative errors in the model's predictions. Fluctuations in rRMSE percentages may suggest differences in the model's predictive accuracy of agricultural waste quantities. Compare the rRMSE percentages of various forecasting models or time periods to determine which has the lowest rRMSE percentage, indicating the best accurate predictions relative to mean real agricultural waste levels. The proposed GECMA-AWRT-RDCNNmethod attains 18.0%, 13.5%, and 11.5%lower Relative Root Mean Squared Errorestimated to the existing method such as PGHGA-LSTM, PAEM-ARIMA and EP-GHGE-SVM models respectively.

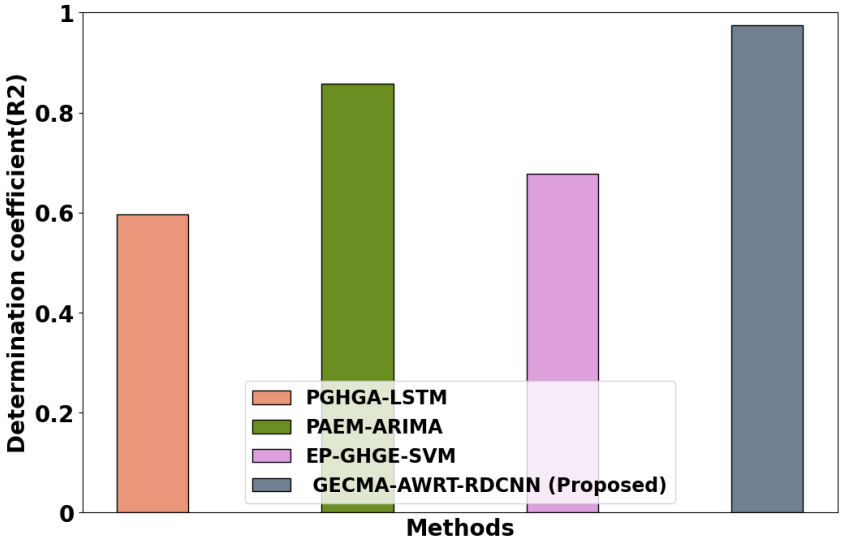

Figure 8: Performance Analyses of Determination Coefficient

Figure 8 displays performance Analyses of Determination Coefficient.Determination Coefficient values can be interpreted as the percentage of variance in agricultural waste quantities that the model can explain. A larger percentage in the Determination Coefficient graph suggests that the model can better account for the variation in agricultural waste quantities. A lower percentage, on the other hand, indicates that the model may not capture all of the data's volatility. The proposed GECMA-AWRT-RDCNNmethod attains 26.0%, 23.5%, and 28.5%higher Determination Coefficientestimated to the existing method such as PGHGA-LSTM, PAEM-ARIMA and EP-GHGE-SVM models respectively.

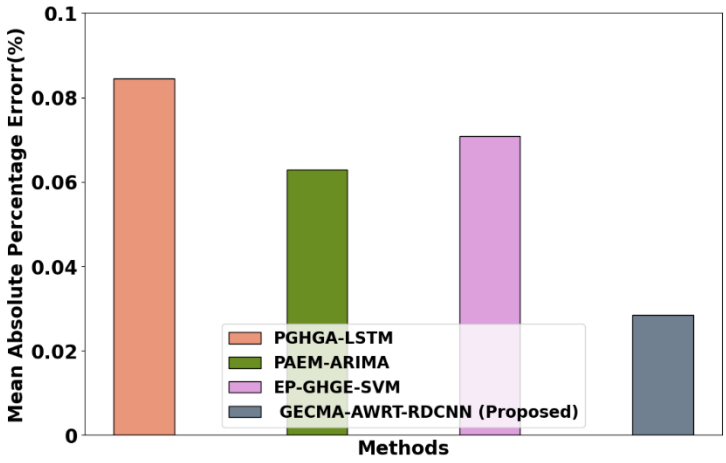

Figure 9: Performance Analysis of Mean Absolute Percentage Error

Figure 9 displays performance analysis of Mean Absolute Percentage Error.The MAPE graph typically depicts MAPE values over time or various data points pertaining to agricultural waste quantities. Each data point on the graph reflects the percentage error between projected and actual values for a given time period or observation. A lower percentage in the MAPE graph indicates that the forecasting model is more accurate in estimating agricultural waste levels. In contrast, a higher percentage indicates a larger average error in the model's predictions. The proposed GECMA-AWRT-RDCNNmethod attains 16.0%, 13.5%, and 18.5%higher Mean Absolute Percentage Errorestimated to the existing method such as PGHGA-LSTM, PAEM-ARIMA and EP-GHGE-SVM models respectively.

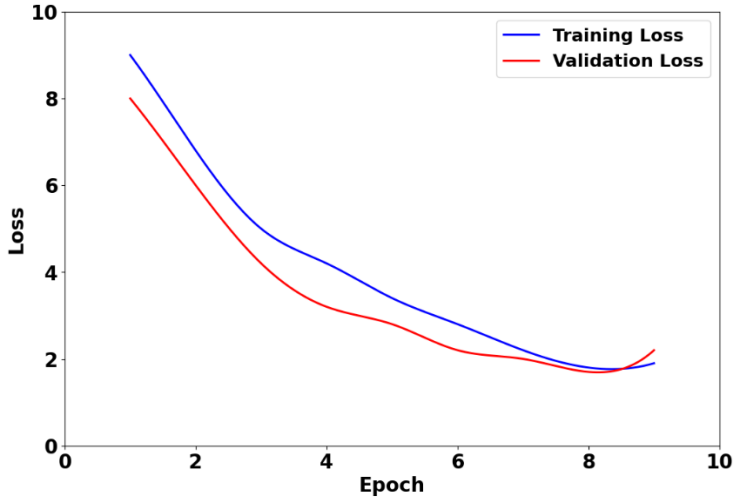

Figure 10: Performance Analyses of Loss

Figure 10 displays performance analyses of Loss.This shows that using RDCNN to optimize the loss function improves performance in forecasting losses related with agricultural waste gas emissions, demonstrating its effectiveness in decreasing environmental impact through more accurate modeling and prediction. The proposed GECMA-AWRT-RDCNNmethod attains 12.0%, 13.5%, and 14.5%lower loss estimated to the existing method such as PGHGA-LSTM, PAEM-ARIMA and EP-GHGE-SVM models respectively.

C. Discussion

Gas emission characterization and monitoring algorithm in the process of agricultural waste resource treatment (GECMA-AWRT-RDCNN)is developed in this research.Countries and metropolitan regions are very concerned about agricultural waste. If not treated correctly, it has a negative impact on both humans and the environment. Recycling and recovering energy from agricultural waste is thought to be a practical way to increase the amount of renewable energy that countries produce, minimize their negative effects on the environment, and produce cleaner products overall. To reduce surplus hazardous gases, like hydrogen (H), nitrogen (N) oxygen (O), sodium(S) and carbon(C), improve energy efficiency, the recycling and recovery of energy from agricultural waste should be precisely forecasted. Consequently, GECMA-AWRT-RDCNNwas created and presented in this

research in order to accurately forecast GY produced by energy recovery from agricultural waste. With the use of this model, agricultural waste processing facilities can precisely forecast the volume of gas yield that would be extracted from agricultural waste sources, enabling them to strategically distribute and adapt their energy resources. Additionally, in order to optimize GYs and prevent the release of surplus hazardous gases into the surrounding environment, the suggested GECMA-AWRT-RDCNN model may be taken into consideration for component adjustment. The derived findings showed that the suggested GECMA-AWRT-RDCNN model was accurate and consistent in forecasting GY produced by energy recovery from agricultural waste. By changing the input parameters, this model can assist the gasification process operates better (i.e., C, H, N, S, Oand Temp). Temp and H have the highest importance based on the inputs' importance scores. These research investigations suggest that by modifying the input variables with high relevance scores, the gasification performance can be enhanced. The proposed GECMA-AWRT-RDCNN model attains higher accuracy 99.9%comparing with existing methods like PGHGA-LSTM, PAEM-ARIMA and EP-GHGE-SVM methods correspondingly.

V. CONCLUSION

In this section, Gas emission characterization and monitoring algorithm in the process of agricultural waste resource treatment (GECMA-AWRT-RDCNN)is successfully implemented. The proposed GECMA-AWRT-RDCNN approach is implemented in Python. The performance of the proposed GECMA-AWRT-RDCNN technique contains 28.0%, 27.5%, and 26.5% higher accuracy, 26.0%, 23.5%, and 28.5% higher Determination Coefficient and 12.0%, 17.5%, and 16.5% lower Mean Squared Error when analysed to the existing methods like PGHGA-LSTM, PAEM-ARIMA and EP-GHGE-SVM methods respectively. Future research will estimate farm emissions following application of the regenerative agriculture method and identify changes contributing to emission reduction in order to better understand how regenerative agriculture can impact climate change. Furthermore, for their analyses, the majority of researchers have been using field data for at least three years. The satellite or picture data can also be used to track greenhouse gas emissions from agriculture.

REFERENCES

[1] SaberiKamarposhti, M., Why, N.K., Yadollahi, M., Kamyab, H., Cheng, J. and Khorami, M., 2024. Cultivating a sustainable future in the artificial intelligence era: A comprehensive assessment of greenhouse gas emissions and removals in agriculture. *Environmental Research*, p.118528.

[2] Maraveas, C., Karavas, C.S., Loukatos, D., Bartzanas, T., Arvanitis, K.G. and Symeonaki, E., 2023. Agricultural greenhouses: Resource management technologies and perspectives for zero greenhouse gas emissions. *Agriculture*, *13*(7), p.1464.

[3] Kavanagh, I., Fenton, O., Healy, M.G., Burchill, W., Lanigan, G.J. and Krol, D.J., 2021. Mitigating ammonia and greenhouse gas emissions from stored cattle slurry using agricultural waste, commercially available products and a chemical acidifier. *Journal of Cleaner Production*, *294*, p.126251.

[4] Wang, S. and Wu, Y., 2021. Hyperthermophilic composting technology for organic solid waste treatment: recent research advances and trends. *Processes*, *9*(4), p.675.

[5] Santolini, E., Bovo, M., Barbaresi, A., Torreggiani, D. and Tassinari, P., 2021. Turning agricultural wastes into biomaterials: Assessing the sustainability of scenarios of circular valorization of corn cob in a life-cycle perspective. *Applied Sciences*, *11*(14), p.6281.

[6] Gautam, M. and Agrawal, M., 2021. Greenhouse gas emissions from municipal solid waste management: A review of global scenario. *Carbon footprint case studies: municipal solid waste management, sustainable road transport and carbon sequestration*, pp.123-160.

[7] Singh, R., Paritosh, K., Pareek, N. and Vivekanand, V., 2022. Integrated system of anaerobic digestion and pyrolysis for valorization of agricultural and food waste towards circular bioeconomy. *Bioresource technology*, *360*, p.127596.

[8] Kumar, M., Ambika, S., Hassani, A. and Nidheesh, P.V., 2023. Waste to catalyst: role of agricultural waste in water and wastewater treatment. *Science of The Total Environment*, *858*, p.159762.

[9] Vazquez-Rowe, I., Ziegler-Rodriguez, K., Margallo, M., Kahhat, R. and Aldaco, R., 2021. Climate action and food security: Strategies to reduce GHG emissions from food loss and waste in emerging economies. *Resources, Conservation and Recycling*, *170*, p.105562.

[10] Thomas, B.S., Yang, J., Mo, K.H., Abdalla, J.A., Hawileh, R.A. and Ariyachandra, E., 2021. Biomass ashes from agricultural wastes as supplementary cementitious materials or aggregate replacement in cement/geopolymer concrete: A comprehensive review. *Journal of Building Engineering*, *40*, p.102332.

[11] Awogbemi, O., Von Kallon, D.V. and Aigbodion, V.S., 2021. Trends in the development and utilization of agricultural wastes as heterogeneous catalyst for biodiesel production. *Journal of the Energy Institute*, *98*, pp.244-258.

[12] Mengqi, Z., Shi, A., Ajmal, M., Ye, L. and Awais, M., 2021. Comprehensive review on agricultural waste utilization and high-temperature fermentation and composting. *Biomass Conversion and Biorefinery*, pp.1-24.

[13] Babu, S., Rathore, S.S., Singh, R., Kumar, S., Singh, V.K., Yadav, S.K., Yadav, V., Raj, R., Yadav, D., Shekhawat, K. and Wani, O.A., 2022. Exploring agricultural waste biomass for energy, food and feed production and pollution mitigation: A review. *Bioresource Technology*, *360*, p.127566.

[14] Møller, H.B., Sørensen, P., Olesen, J.E., Petersen, S.O., Nyord, T. and Sommer, S.G., 2022. Agricultural biogas production—climate and environmental impacts. *Sustainability*, *14*(3), p.1849.

[15] Suhartini, S., Nurika, I., Paul, R. and Melville, L., 2021. Estimation of biogas production and the emission savings from anaerobic digestion of fruit-based agro-industrial waste and agricultural crops residues. *BioEnergy Research*, *14*(3), pp.844-859.

[16] Kumar Sarangi, P., Subudhi, S., Bhatia, L., Saha, K., Mudgil, D., Prasad Shadangi, K., Srivastava, R.K., Pattnaik, B. and Arya, R.K., 2023. Utilization of agricultural waste biomass and recycling toward circular bioeconomy. *Environmental Science and Pollution Research*, *30*(4), pp.8526-8539.

[17] Karić, N., Maia, A.S., Teodorović, A., Atanasova, N., Langergraber, G., Crini, G., Ribeiro, A.R. and Đolić, M., 2022. Bio-waste valorisation: Agricultural wastes as biosorbents for removal of (in) organic pollutants in wastewater treatment. *Chemical Engineering Journal Advances*, *9*, p.100239.

[18] Rani, G.M., Pathania, D., Umapathi, R., Rustagi, S., Huh, Y.S., Gupta, V.K., Kaushik, A. and Chaudhary, V., 2023. Agro-waste to sustainable energy: A green strategy of converting agricultural waste to nano-enabled energy applications. *Science of The Total Environment*, *875*, p.162667.

[19] Smith, P., Reay, D. and Smith, J., 2021. Agricultural methane emissions and the potential formitigation. *Philosophical Transactions of the Royal Society A*, *379*(2210), p.20200451.

[20] Siddiki, S.Y.A., Uddin, M.N., Mofijur, M., Fattah, I.M.R., Ong, H.C., Lam, S.S., Kumar, P.S. and Ahmed, S.F., 2021. Theoretical calculation of biogas production and greenhouse gas emission reduction potential of livestock, poultry and slaughterhouse waste in Bangladesh. *Journal of Environmental Chemical Engineering*, *9*(3), p.105204.

[21] Kosamkar, P.K. and Kulkarni, V.Y., 2021. Role of deep learning for prediction of greenhouse gas emission from agriculture: enabling technology. International Journal of Agriculture Innovation, Technology and Globalisation, 2(2), pp.97-107.

[22] Homaira, M. and Hassan, R., 2021. Prediction of Agricultural Emissions in Malaysia Using Machine Learning Algorithms. International Journal on Perceptive and Cognitive Computing.

[23] Bakay, M.S. and Ağbulut, Ü., 2021. Electricity production based forecasting of greenhouse gas emissions in Turkey with deep learning, support vector machine and artificial neural network algorithms. Journal of Cleaner Production, 285, p.125324.

[24] Nielsen, C.K., Elsgaard, L., Jørgensen, U. and Lærke, P.E., 2023. Soil greenhouse gas emissions from drained and rewetted agricultural bare peat mesocosms are linked to geochemistry. Science of the Total Environment, 896, p.165083.

[25] Raihan, A., Muhtasim, D.A., Farhana, S., Hasan, M.A.U., Pavel, M.I., Faruk, O., Rahman, M. and Mahmood, A., 2023. An econometric analysis of Greenhouse gas emissions from different agricultural factors in Bangladesh. Energy Nexus, 9, p.100179.

[26] Gołasa, P., Wysokiński, M., Bieńkowska-Gołasa, W., Gradziuk, P., Golonko, M., Gradziuk, B., Siedlecka, A. and Gromada, A., 2021. Sources of greenhouse gas emissions in agriculture, with particular emphasis on emissions from energy used. Energies, 14(13), p.3784.

[27] Sharafi, S., Kazemi, A. and Amiri, Z., 2023. Estimating energy consumption and GHG emissions in crop production: A machine learning approach. Journal of Cleaner Production, 408, p.137242.

[28] https://www.kaggle.com/datasets/alessandrolobello/agri-food-co2-emission-dataset forecasting-ml?select=Agrofood_co2_emission.csv

[29] NajianAsl, R. and Bletzinger, K.U., 2023. The implicit bulk-surface filtering method for node-based shape optimization and a comparison of explicit and implicit filtering techniques. Structural and Multidisciplinary Optimization, 66(5), p.111.

[30] Wang, H. and Zhao, J., 2023. A novel high-level target navigation pigeon-inspired optimization for global optimization problems. *Applied Intelligence*, *53*(12), pp.14918-14960.

[31] Zhang, Q., Xiao, J., Tian, C., Chun-Wei Lin, J. and Zhang, S., 2023. A robust deformed convolutional neural network (CNN) for image denoising. CAAI Transactions on Intelligence Technology, 8(2), pp.331-342.

[32] Tang, Z., Wang, K., Zang, Y., Zhu, Q., Todo, Y. and Gao, S., 2024. Fractional-Order Water Flow Optimizer. *International Journal of Computational Intelligence Systems*, *17*(1), p.84.